Identification of a Brain Penetrant PDE9A Inhibitor Utilizing Prospective Design and Chemical Enablement as a Rapid Lead Optimization Strategy

Patrick R. Verhoest,* Caroline Proulx-Lafrance, Michael Corman, Lois Chenard, Christopher J. Helal, Xinjun Hou, Robin Kleiman, Shenping Liu, Eric Marr, Frank S. Menniti, Christopher J. Schmidt, Michelle Vanase-Frawley, Anne W. Schmidt, Robert D. Williams, Frederick R. Nelson, Kari R. Fonseca, and Spiros Liras*

Neuroscience Chemistry, Pfizer Global Research and Development, Eastern Point Road, Groton, Connecticut 06340

Abstract: By use of chemical enablement and prospective design, a novel series of selective, brain penetrant PDE9A inhibitors have been identified that are capable of producing in vivo elevations of brain cGMP.

Members of the phosphodiesterase (PDE[a]) gene family are widely and abundantly expressed in the brain.[1] On the basis of the physiological importance of cyclic nucleotide signaling in the central nervous system (CNS) and the therapeutic potential for restoration of dysfunctional neuronal signaling cascades via PDE inhibition, we launched an initiative to identify potential therapeutic utility for several CNS disorders. An attractive feature of the PDE neuroscience discovery platform was the apparent drug-ability of the gene family.[2] We have previously disclosed the discovery of several novel classes of selective PDE10A inhibitors,[3] including the discovery of PF-2545920 (**1**), a selective PDE10A inhibitor that has entered clinical development for the treatment of schizophrenia.[4]

Here we report our subsequent efforts to identify and optimize selective PDE9A inhibitors. PDE9A is a high affinity cGMP-specific PDE expressed in the brain.[5] The high affinity for cGMP (K_m = 170 nM) relative to all other PDE enzymes suggests a physiological role in modulation of cGMP in a lower cytoplasmic cGMP concentration range than any other PDE.[6] Our main objective was to identify selective pharmacological tools that would allow us to establish confidence in the biological hypothesis that PDE9A inhibition will treat cognitive deficits.[7] It has been reported that cGMP can reverse Aβ induced deficits in long-term potentiation in hippocampal slices[8] and improve cognition in behavioral studies.[9] We hypothesize that inhibition of the enzyme will elevate cGMP and improve synaptic transmission, stabilize vulnerable

Figure 1. Comparison of key properties for sildenafil and **1** vs **2**.
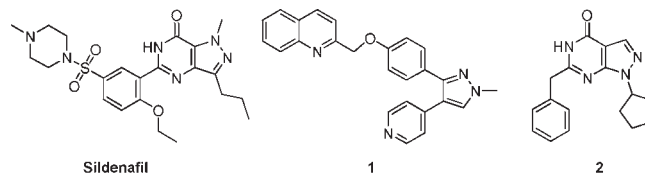
	Sildenafil	1	2
MW	475	392	294
NO Count	10	5	5
ClogP	1.98	3.94	2.34
TPSA	113	52	64
HBond donor	1	0	1

synapses, and ultimately lead to an improvement in cognitive deficits observed in patients with Alzheimer's disease.

The Pfizer neuroscience PDE platform represents a valuable opportunity to capitalize on the accumulated company experience from the discovery of Sildenafil and subsequently from the prosecution of the PDE10A program. We developed a chemistry strategy for the prosecution of additional members of the PDE family of interest to neuroscience. The strategy was based on the principles of prospective design and chemical enablement. Prospective design enables us to probe in tandem multiple layers of hypotheses for lead optimization based on knowledge. Chemical enablement is the efficient bond disconnection that facilitates the synthesis of libraries that probe multiple hypotheses. This strategy enabled the rapid parallel optimization of multiple lead options.

Internal screening efforts and in silico ADME assessment yielded one brain penetrating chemical series of interest depicted in Figure 1. The screening hit **1** possessed numerous attractive features including high affinity for PDE9A (2.1 nM), low molecular weight (<300), high ligand efficiency (LE = 0.53),[10] and a brain to plasma ratio (*B*/*P*) of 1.2. This lead was plagued by numerous liabilities such as high clearance, poor selectivity across multiple PDEs (PDE1C 2.1 nM), and low solubility.

To optimize clearance and retain high exposure in the CNS, we focused our design plan on a set of key molecular properties identified as critical based on the PDE10A project conclusions. For example, the PDE10A candidate (**1**) achieved appreciable brain exposure with a molecular weight of <400 and a modest N/O count. Other quinazoline PDE10A inhibitors were able to achieve brain penetration with higher TPSA[11] (83) and lower ClogP. The key to their central access was that unlike many CNS drugs, they do not possess a strongly basic nitrogen, and they minimize molecular weight and hydrogen bond donor count.

In contrast, sildenafil, which demonstrates modest ability to enter the CNS,[12] is characterized by a higher molecular weight, a high count of N/O atoms (resulting in an elevated TPSA), and a hydrogen bond donor. Thus, the guiding principles for aligning clearance, CNS disposition, and safety[13] were postulated to be maintaining molecular weight under 430 and ClogP under 3.0, limiting the number of H bond donor atoms to 1, and targeting TPSA in the spectrum between 50 and 100.

*To whom correspondence should be addressed. For P.R.V.: phone, 860-686-2288; fax, 860-686-0013; e-mail, patrick.r.verhoest@pfizer.com. For S.L.:, phone, 860-441-1739; fax, 860-715-8224; e-mail, spiros.liras@pfizer.com.
[a] Abbreviations: PDE, phosphodiesterase; cGMP, cyclic guanosine monophosphate; CNS, central nervous system; SBDD, structure based drug design.

The second objective was to develop a strategy for the rapid delivery of tools with adequate exposure to trigger pharmacodynamic effects. Pharmacodynamic effects were observed at free plasma or CSF exposures that corresponded to approximately 5 times the IC_{50} in previous projects targeting PDE5[14] and PDE10A. Our aim was to maintain potency and optimize free fraction, in vivo efficacy, and improve the metabolic profile in parallel by reducing lipophilicity. We expected these modifications would increase plasma and brain free fraction.[15]

Our final objective was to devise a synthesis plan that would allow us to meet our design objectives with a minimum number of design-synthesis cycles. Thus, we built an innovative synthesis plan to probe in tandem a range of substitutions for both the pyrazole carbocycle and the pyrimidinone benzyl group. We developed a plate-based chemistry approach for the parallel manipulation of two vectors which is depicted in Scheme 1.

Scheme 1. Core Parallel Synthesis
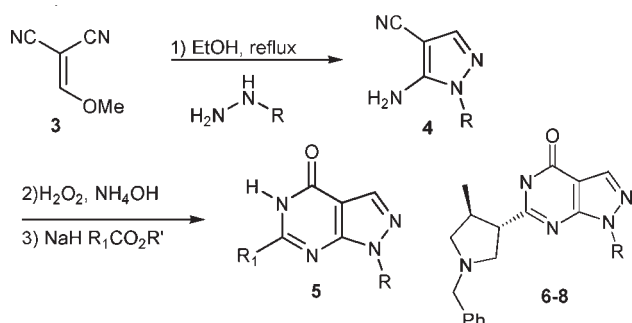
Synthetically, the dicyano electrophile **3** could be coupled with a variety of hydrazines to afford pyrazoles. The remaining cyano group could be oxidized in the presence of a large number of functional groups with 30% peroxide in aqueous ammonium hydroxide. Cyclization with esters proceeded in dioxane with sodium hydride as the base followed by addition of *n*-BuOH and heating to provide the desired pyrazolopyrimidines. This parallel protocol produced 50% of the designed molecules in high purity for testing.

The power of the chemical enablement allowed us to consider making 89 000 compounds based on the commercially and internally available hydrazines and esters. With the large potential pool of compounds to synthesize we developed a strategy for filtering our monomers and potential products. By filtering the hydrazine and ester monomers sets to MW < 220 and by excluding monomers with additional hydrogen bond donors, we expected to synthesize molecules with desirable CNS penetration. As part of our monomer selection, we also included all parallel enabled monomers, i.e., monomers that could provide an additional handle for future library chemistry and rapid SAR optimization. Many enabled monomers contain a basic nitrogen that would aid in solubility. We anticipated that the insertion of a basic center was likely to invite additional issues such as PgP efflux, 2D6 metabolism,[16] and interaction with HERG.[17] However, the parallel chemistry enabled monomers would allow us to rapidly explore the optimal basic pK_a range to alleviate these problems.

Filtering the monomers provided 3500 potential compounds for synthesis. Selecting the final compounds based on the physicochemical properties of ClogP < 3, TPSA < 110, and MW < 430 provided 2400 compounds for consideration.
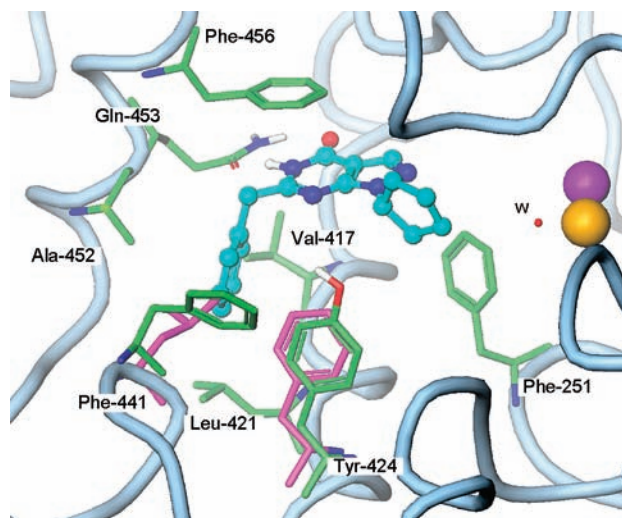

Figure 2. PDE9A inhibitor **2** (PDB 3JS1) bound and structural differences with PDE1C (pink).

The crystal structure of the lead inhibitor **2** (Figure 2) showed that the pyrimidinone made a two-point hydrogen bond interaction with the conserved glutamine (Gln-453) similar to the known PDE5 inhibitors. The benzyl group is situated in a lipophilic pocket formed by Val-417, Leu-421, Phe-441, and Ala-452. Utilizing the PDE9A crystal structure of **2** and a homology model of PDE1C, we developed a strategy for targeting the two residues that are distinct and in proximity to the conserved glutamine.[18] PDE9A contains Tyr-424, a unique residue within the PDE family. In PDE1C and most other PDEs this position contains a phenylalanine. We envisioned that a ligand interacting with the tyrosine would increase its selectivity for PDE9. We anticipated that increasing selectivity through a polar interaction would also improve our druglike properties. The second PDE9A residue, Phe-441, which is an alanine in PDE1C, could also provide an opportunity for an aromatic π-stacking interaction. Utilizing this knowledge, we docked[19] the 2400 compounds from our virtual library into the PDE9A binding pocket with the pyrazolopyrimidine core partially constrained as in the X-ray structure of **2**. These docked compounds were scored using an in-house scoring method.[20] We chose to synthesize the top ranking compounds (500) based on scoring and visual inspections by focusing on the compound's ability to form a hydrogen bond interaction with Tyr-424 and a π-stacking interaction with Phe-441.

From this effort we identified a key ester precursor shown in **6**−**8**. The library containing this pyrrolidine benzyl group afforded compounds with improved selectivity over PDE1C (Table 1).

Table 1. PDE9A and PDE1C IC_{50} in nM

#	R	PDE9A	PDE1C
6		150	1500
7		66	2100
8		63	971

The pyrrolidine group of **8** improved selectivity 15-fold compared to the initial lead **2**. We acquired an X-ray crystal structure of **7** bound in PDE9A. The design concept of
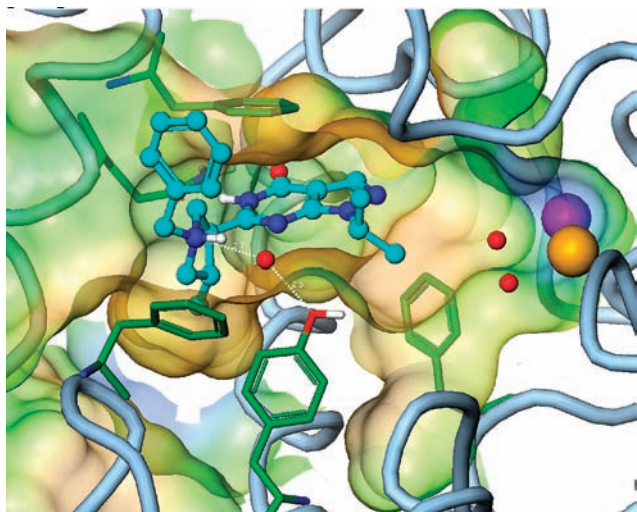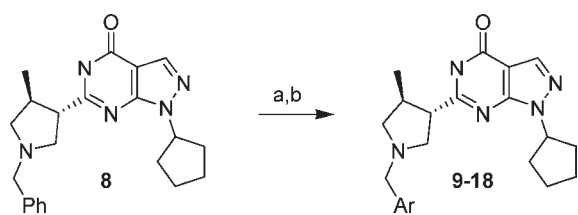
Figure 3. PDE9A inhibitor **7** bound in PDE9A making key interactions to Tyr-424 (PDB 3JSW).

Scheme 2[a]

[a] (a) H$_2$, Pd/C, EtOH (57%); (b) NaCNBH$_3$, parallel chemistry.

Table 2. PDE9A and PDE1C IC$_{50}$ in nM

#	Ar	PDE9A	PDE1C
9		40	563
10		200	1300
11		29	270
12		16	190
13		11	400
14		15	210
15		11	200
16		11	110
17		12	220
18		2	73

hydrogen bonding to Tyr-424 had come to fruition. The pyrrolidine nitrogen of **7** hydrogen bonds to Tyr-424 through a water molecule, representing a slight deviation from our projected docking model. In addition, the benzyl group has multiple conformations and shows density in the X-ray structure consistent with an edge on interaction with Phe-456 and a π-stack interaction with Phe-441, just as designed. The methyl group on the pyrrolidine partially filled the lipophilic pocket that was occupied by the benzyl group of **2**.

The major advantage of selecting enabled monomers was evidenced by the identification of **8**. We were able to rapidly synthesize **8** on scale and remove the benzyl group via hydrogenation. This allowed us to utilize parallel chemistry for the second time to conduct a reductive amination library with a variety of aromatic and heteroaromatic aldehydes. This monomer flexibility permitted us to rapidly explore the SAR and to modulate the physicochemical properties of our inhibitors. The heteroaryls provided compounds with decreased lipophilicity and reduced the pK_a of the pyrrolidine.

The reductive amination library exemplified in Table 2 showed that this series has inherent PDE9A selectivity. On average each compound was at least 10-fold selective. The SAR of the aromatic ring was very flexible in that it tolerated 5- and 6-member heterocycles along with substituents that were electron withdrawing or donating. In addition, 10-member bicyclic aromatic groups, such as **18**, provided excellent potency (2 nM) and selectivity > 30×. This is potentially a result of a better edge-on interaction with Phe-456 of PDE9A.

Compound **18** exhibited the desired in vitro profile, triggering separation of the enantiomers. On the basis of the X-ray structure (Figure 3), we determined which enantiomer would possess the majority of the activity. We were able to separate **8** via preparative chiral chromatography. Following Scheme 2 we were able to prepare both enantiomers of **18**.

Compound **19** (PF-4181366, Figure 4) showed PDE9A affinity of 1.8 nM with > 25× selectivity. The less active enantiomer displayed a PDE9 IC$_{50}$ of 50 nM. Compound **19** displayed the in vitro profile we were targeting for a tool compound to build our confidence in rationale for Alzheimer's disease.
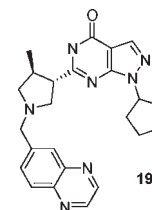

Figure 4. Active enantiomer **19**.

Compound **19** was dosed in rodents to understand the potential for CNS penetration. By design, this compound had a weakly basic pK_a, minimal MW, and a limited number of hydrogen bond donors which resulted in excellent central exposure with no PgP liability. The brain to plasma ratio in a rat was 1.4 and the free drug exposure equaled the CSF exposure, suggesting **19** has no barriers to CNS penetration.

Compound **19** elevated cGMP in the striatum of mice in a dose responsive fashion (Figure 5). A 145% elevation occurred at 3.2 mg/kg, and at 10 mg/kg a 215% elevation was
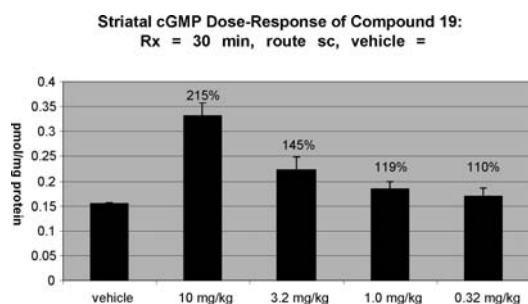

Figure 5. Dose responsive increase in striatal cGMP with **19**.

observed. As predicted from experience with other PDE targets, we saw a physiological effect at ∼5× the PDE9 IC_{50} in the CSF.

Overall, **19** exhibited all the attributes of a pharmacological tool that could be used to build confidence in the biological rationale of the target. Delivery of this compound validated our lead optimization strategy which was built upon knowledge management, prospective design, and chemical enablement. Future publications will detail the advancement of this series and identification of a PDE9i clinical candidate.

Supporting Information Available: Chemistry, biology, and pharmacokinetics experimental descriptions and data. This material is available free of charge via the Internet at http://pubs.acs.org.

References

(1) Menniti, F. S.; Faraci, S. W.; Schmidt, C. J. Phosphodiesterases in the CNS: Targets for Drug Development. *Nat. Rev. Drug Discovery* **2006**, *5* (8), 660–670.

(2) Setter, S. M.; Iltz, J. L.; Fincham, J. E.; Campbell, R. K.; Baker, D. E. Phosphodiesterase 5 Inhibitors for Erectile Dysfunction. *Ann. Pharmacol.* **2005**, *39* (7/8), 1286–1295.

(3) Chappie, T. A.; Humphrey, J. M.; Allen, M. P.; Estep, K. G.; Fox, C. B.; Lebel, L. A.; Liras, S.; Marr, E. S.; Menniti, F. S.; Pandit, J.; Schmidt, C. J.; Tu, M.; Williams, R. D.; Yang, F. V. Discovery of a Series of 6,7-Dimethoxy-4-pyrrolidylquinazoline PDE10A Inhibitors. *J. Med. Chem.* **2007**, *50* (2), 182–185.

(4) Verhoest, P. R.; Chapin, D. S.; Corman, M.; Fonseca, K.; Harms, J. F.; Hou, X.; Marr, E. S.; Menniti, F. S.; Nelson, F.; O'Connor, R.; Pandit, J.; Proulx-LaFrance, C.; Schmidt, A. W.; Schmidt, C. J.; Suiciak, J. A.; Liras, S. Discovery of a Novel Class of PDE10A Inhibitors and Identification of Clinical Candidate 2-[4-(1-Methyl-4-pyridin-4-yl-1*H*-pyrazol-3-yl)phenoxy methyl]-quinoline (PF-2545920) for the Treatment of Schizophrenia. *J. Med. Chem.* **2009**, *52* (16), 5188–5196.

(5) Andreeva, S. G.; Dikkes, P.; Epstein, P. M.; Rosenberg, P. A. Expression of cGMP-Specific Phosphodiesterase 9A mRNA in the Rat Brain. *J. Neurosci.* **2001**, *21* (22), 9068–9076.

(6) Fisher, D. A.; Smith, J. F.; Pillar, J. S.; St. Denis, S. H.; Cheng, J. B. Isolation and Characterization of PDE9A, a Novel Human cGMP-Specific Phosphodiesterase. *J. Biol. Chem.* **1998**, *25* (273), 15559–15564.

(7) Van Der Staay, F. J.; Rutten, K.; Barfacker, L.; DeVry, J.; Erb, C.; Schroder, H. H.; Hendrix, M. The Novel Selective PDE9 Inhibitor BAY 73-6691 Improves Learning and Memory in Rodents. *Neuropharmacology* **2008**, *55* (5), 908–918.

(8) Puzzo, D.; Vitolo, O.; Fabrizio, T.; Jacob, J. P.; Palmeri, A.; Arancio, O. Amyloid-beta Peptide Inhibits Activation of the Nitric Oxide/cGMP/cAMP Responsive Element-Binding Protein Pathway during Hippocampal Synaptic Plasticity. *J. Neurosci.* **2005**, *25* (29), 6887–6897.

(9) Prickaerts, J.; Steinbusch, H. W.; Smits, J. F. M.; De Vente, J. Possible Role of Nitric Oxide-Cyclic GMP Pathway in Object Recognition Memeory: Effects of 7-Nitroindazole and Zaprinast. *Eur. J. Pharmacol.* **1997**, *337* (2/3), 125–136.

(10) Hopkins, A. L.; Groom, C. R.; Alex, A. Ligand Efficiency: A Useful Metric for Lead Selection. *Drug Discovery Today* **2004**, *9* (10), 430–431.

(11) Ertl, P.; Rohde, B.; Selzer, P. Fast Calculation of Molecular Polar Surface Area as a Sum of Fragment-Based Contributions and Its Applications to the Prediction of Drug Transport Properties. *J. Med. Chem.* **2000**, *43* (20), 3714–3717.

(12) Walker, D. K.; Ackland, M. J.; James, G. C.; Muirhead, G. J.; Rance, D. J.; Wastall, P.; Wright, P. A. Phamacokinetics and Metabolism of Sildenafil in Mouse, Rat, Rabbit, Dog and Man. *Xenobiotica* **1999**, *29* (3), 297–310.

(13) Hughes, J. D.; Blagg, J.; Price, D. A.; Bailey, S.; DeCrescenzo, G. A.; Devraj, R. V.; Ellsworth, E.; Fobian, Y. M.; Gibbs, M. E.; Gilles, R. W.; Greene, N.; Huang, E.; Krieger-Burke, T.; Loesel, J.; Wager, T.; Whiteley, L.; Zhang, Y. Physiochemical Drug Properties Associated with in Vivo Toxicological Outcomes. *Bioorg. Med. Chem. Let.* **2008**, *18* (17), 4872–4875.

(14) Govier, F.; Potempa, A.; Kaufman, J.; Denne, J.; Kovalenko, P.; Ahuja, S. A Multicenter, Randomized, Double-Blind, Crossover Study of Patient Preference for Tadalafil 20 mg or Sildenafil Citrate 50 mg during Initiation of Treatment for Erectile Dysfunction. *Clin. Ther.* **2003**, *25* (11), 2709–2723.

(15) Summerfield, S. G.; Read, K.; Begley, D. J.; Obradovic, T.; Hidalgo, I. J.; Coggon, S.; Lewis, A. V.; Porter, R. A.; Jeffrey, P. Central Nervous System Drug Deposition: The Relationship between in Situ Brain Permeability and Brain Free Fraction. *J. Pharmacol. Exp. Ther.* **2007**, *322* (1), 205–213.

(16) De Groot, M. J.; Ackland, M. J.; Horne, V. A.; Alex, A. A.; Jones, B. C. Novel Approach to Predicting P450-Mediated Drug Metabolism: Development of a Combined Protein and Pharmacophore Model for CYP2D6. *J. Med. Chem.* **1999**, *42* (9), 1515–1524.

(17) Murphy, S. T.; Case, H. L.; Ellsworth, E.; Hagen, S.; Huband, M.; Joannides, T.; Limberakis, C.; Marotti, K. R.; Ottolini, A. M.; Rauckhorst, M.; Starr, J.; Stier, M.; Taylor, C.; Zhu, T.; Blaser, A.; Denny, W. A.; Lu, G.; Small, J.; Rivault, F. The Synthesis and Biological Evaluation of Novel Series of Nitrile-Containing Fluoroquinolones as Antibacterial Agents. *Bioorg. Med. Chem. Lett.* **2007**, *17* (8), 2150–2155.

(18) Card, G. L.; England, B. P.; Suzuki, Y.; Fong, D.; Powell, B.; Lee, B.; Luu, C.; Tabrizizad, M.; Gillete, S.; Ibrahim, P. N.; Artis, D. R.; Bollag, G.; Milburn, M. V.; Kim, S.; Schlessinger, J.; Zang, K. Y. J. Structural Basis for the Activity of Drugs That Inhibit Phosphodiesterases. *Structure* **2004**, *12*, 2233–2247.

(19) Gehlhaar1, D. K.; Verkhivker1, G. M.; Rejto1, P. A.; Sherman, C. J.; Fogel, D. R.; Fogel, L. J.; Freer, S. T. Molecular Recognition of the Inhibitor AG-1343 by HIV-1 Protease: Conformationally Flexible Docking by Evolutionary Programming. *Chem. Biol.* **1995**, *2*, 317–324.

(20) Marrone1, T. J.; Luty, B. A.; Rose, P. W. Discovering High-Affinity Ligands from the Computationally Predicted Structures and Affinities of Small Molecules Bound to a Target: A Virtual Screening Approach. *Perspect. Drug Discovery Des.* **2000**, *20*, 209–230.